

# Petrology and geochemistry of Upper Proterozoic shales of the Visingsö Group, southern Sweden

SADOON MORAD and BENGT COLLINI

Morad, S. and Collini, B. 1991 06 15: Petrology and geochemistry of Upper Proterozoic shales of the Visingsö Group, southern Sweden. *Bulletin of the Geological Institutions of the University of Uppsala*, N.S., Vol. 16. pp. 61–68. Uppsala. ISSN 0302–2749.

Shale samples collected from alluvial-fan and intertidal-subtidal deposits of the Visingsö Group (Upper Proterozoic; southern Sweden) were studied petrologically and analysed for major and trace elements (Ni, Zn, Pb, Mn, Cr, Sr and Ba). The reddish alluvial-fan shales contain hematite and have higher illitic clay minerals/chlorite ratio than the greenish alluvial-fan shales (3.7 and 2.7, respectively). The intertidal-subtidal shales studied were greyish to black in colour and contain carbonates and pyrite and their average illitic clay minerals/chlorite ratio is 2.3. The mineralogical differences among the shale groups account for the differences in abundance and/or distribution pattern of, particularly,  $\text{Fe}^{2+}$ ,  $\text{Fe}^{3+}$ , Mg, Ca, Mn, Ba and Sr.

S. Morad and B. Collini, Department of Mineralogy and Petrology, Institute of Geology, Uppsala University, Box 555, S-751 22 Uppsala, Sweden, 15th October, 1990.

## Introduction

The Visingsö Group (Upper Proterozoic) consists of unmetamorphosed sedimentary rocks that occur in the area of Lake Vättern and its surroundings in southern Sweden (Fig. 1). The group is comprised of three lithostratigraphic units (Collini 1951): a lower, middle, and upper unit (Fig. 1). Shale samples from the middle unit are reddish and grey-green in colour and represent alluvial-fan deposits that are interbedded with arkosic sandstones. The shale samples studied from the upper unit are grey to black and represent intertidal-subtidal deposits interbedded with carbonate rocks, calcarenites and calcareous sandstones. The lower unit is mainly composed of beach-deposited quartz arenites. The diagenesis of the sandstones has been studied by Morad (1983, 1986) and AlDahan & Morad (1986).

The aims of this paper are to investigate the possible chemical and mineralogical variations of shales in relation to facies and colour and to evaluate the effects of diagenesis on their geochemical evolution.

## Analytical methods

Sixteen reddish coloured and fifteen grey-green coloured shale samples from the middle unit and twenty one shale samples from the upper unit were used in this study. The analyses (performed on bulk

shale samples) of most of the major elements were made following the wet-chemical methods of Kolthoff & Sandell (1959). Concentrations of sodium, potassium and the trace elements were determined by an atomic absorption spectrophotometer. Six representative samples from each shale group were powdered and analysed by  $\text{CuK}_\alpha$  X-ray diffractometer using Ni-filter at a rate of  $1^\circ 2\theta/\text{min}$  for purpose of semiquantitative determination of bulk-mineralogical composition based on measurement of the areas under the peaks. Selected sample chips were coated with a thin layer of gold and examined by a JEOL JSM840 scanning electron microscope (SEM) equipped with an energy dispersive X-ray analyser.

## Results and interpretation

### *Petrography and mineralogy*

The shales studied have dominating particle size that ranges from clay to silt. Thin (0.5–1 mm) inter-laminations of silt and silty clay laminae that usually terminate into clay laminae are common (Fig. 2A). Silt-sized micas occur in the clay laminae and along the clay-silt laminae (Fig. 2B). The clay mineral flakes in the clay laminae are arranged parallel to bedding but bent around fine silt-sized quartz and feldspar grains (Fig. 2C). Shales comprised pre-

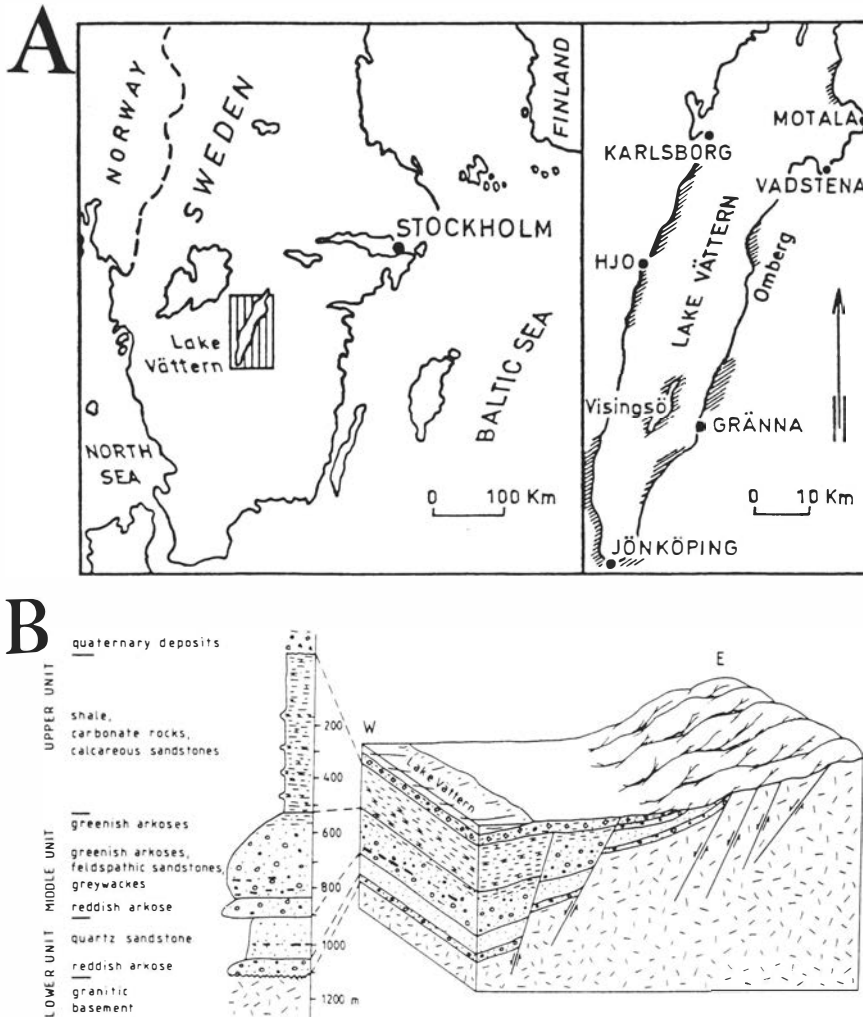


Fig. 1. (A) Location map and outcrops of the Visingsö Group (Shaded area). (B) A general geological setting of the Visingsö Group in the area of Gränna.

Table 1. Average mineral composition of the shales based on X-ray diffraction analyses.

Minerals (vol. %)	RS	GS	ISS
Quartz	35	34	29
Potassium feldspar	5	6	5
Plagioclase	2	2	3
Illitic clay minerals + mica	41	40	35
Chlorite	11	15	15
Kaolinite	4	3	4
Carbonates	trace	trace	8
Pyrite	0.0	trace	1
Hematite	3	trace	0.0

dominantly of clay mineral flakes are characterized by good fissility (cf. Blatt et al. 1980). The mica flakes are commonly etched due to dissolution, oxidized into hematite (in the reddish shales) and replaced by clay minerals (Fig. 3).

The average bulk mineralogical compositions of the shale groups are given in Table 1. Illitic clay minerals (including micas), quartz, chlorite and feldspar are dominant. Potassium feldspars dominate over plagioclase. Carbonates and pyrite occur mainly in the intertidal-subtidal shales (ISS) of the upper unit. The carbonate occurs as authigenic algal precipitated calcite or as micrite/microdolomite dispersed within the clay minerals. Partially dissolved

carbonate intraclasts were also observed (Fig. 4). Authigenic pyrite occurs as aggregates composed of several crystals close to altered biotite (Fig. 5). These pyrite-crystal aggregates represent incompletely developed framboidal texture (Fig. 5B, C); however, true framboidal pyrite occurs too. The grey-green alluvial-fan shales (GS) and to lesser extent the ISS shales have a lower illitic clay/chlorite ratio (2.7 and 2.3, respectively) than the reddish alluvial-fan shales (RS; 3.7). The RS shales are characterized by the presence of extremely fine iron-oxide pigment intermixed or attached to the clay mineral flakes (cf. Caroll 1958).

Although quartz occurs predominantly as detrital grains, trace amounts of authigenic fine-crystalline quartz were detected by means of the SEM examination (Fig. 6). Feldspar grains are slightly pervasively etched (Fig. 7A) and/or replaced by clay minerals (Fig. 7B). Ilmenite and titaniferous magnetite occur as few grains that are altered into Ti-oxides and pyrite (in the ISS and GS samples) or into Fe- and Ti-oxides (in the RS samples) (Morad & AlDahan 1986).

#### Major and trace element chemistry

By way of introduction, it should be borne in mind that the correlations between the major elements discussed below represent a closed system. Caution must be taken when interpreting them.

The average chemical composition reveals differences in major and trace element contents between the three groups of shales (Table 2).  $\text{SiO}_2$  is highest in the RS shales due to the higher content of quartz and illitic clay minerals. The low  $\text{SiO}_2$  content in the ISS shales is due to the presence of higher amounts of carbonate minerals than in the other shale groups. The positive correlation of  $\text{TiO}_2$  with  $\text{Al}_2\text{O}_3$ ,  $\text{K}_2\text{O}$  and  $\text{Fe}_2\text{O}_3$  in the GS and RS shales (Tables 3 and 4) suggest that Ti is mostly allocated in the illitic clay minerals and mica.  $\text{TiO}_2$  is also present as fine-crystalline Ti-oxides and occurs in detrital Fe-Ti oxides. The amounts of  $\text{Al}_2\text{O}_3$  which resides in the clay minerals and feldspars, is negatively correlated with  $\text{SiO}_2$  (mainly as quartz) particularly in the RS and GS shales (Tables 3 and 4) and with CaO (i.e., carbonates) in the ISS shales (Table 5).

One very obvious difference between the shale groups is the  $\text{Fe}_2\text{O}_3$  and FeO contents. Although the total iron content does not vary considerably within the three shale groups, the  $\text{Fe}_2\text{O}_3/\text{FeO}$  ratio is much lower in the ISS (0.5) and GS (0.6) shales than in the RS shales (2.9). This difference is related to the presence of hematite and, to a small

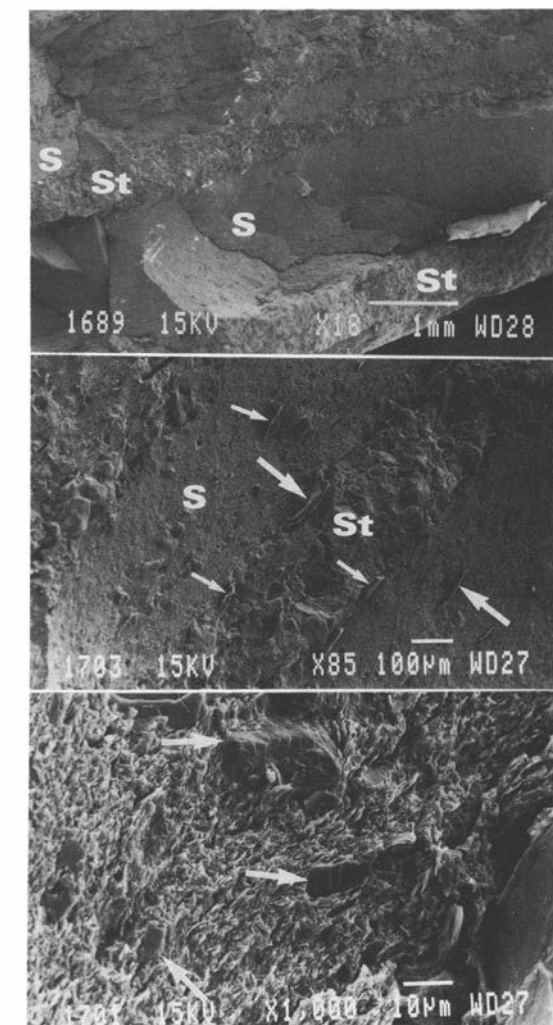


Fig. 2. SEM micrographs showing: (A) microinterlamination of clay-rich (S) and silt-rich (St) laminae in a shale sample from the distal-fan deposits. (B) The same feature as in Fig. 2A but revealing the presence of parallel aligned mica flakes (arrows) in the clay-rich laminae and at the upper and lower surfaces of a silt-rich layer bounded by clay-rich layers. (C) Part of the clay-rich layer in Fig. 2B shown at higher magnification to show the parallel alignment of the clay mineral flakes and their local bending (arrows) around the fine silt-sized quartz and feldspar grains.

extent, more illitic clay minerals (notice the positive correlation between  $\text{Fe}_2\text{O}_3$  and  $\text{K}_2\text{O}$  in tables 3 and 4) in the RS shales. The lower  $\text{Fe}_2\text{O}_3/\text{FeO}$  ratio in the GS and ISS shales is related to the more abundant pyrite and chlorite. However, the weak correlation coefficient of FeO with MgO and  $\text{Al}_2\text{O}_3$  in the ISS (Table 5) shales suggests that FeO substantially occurs as pyrite.

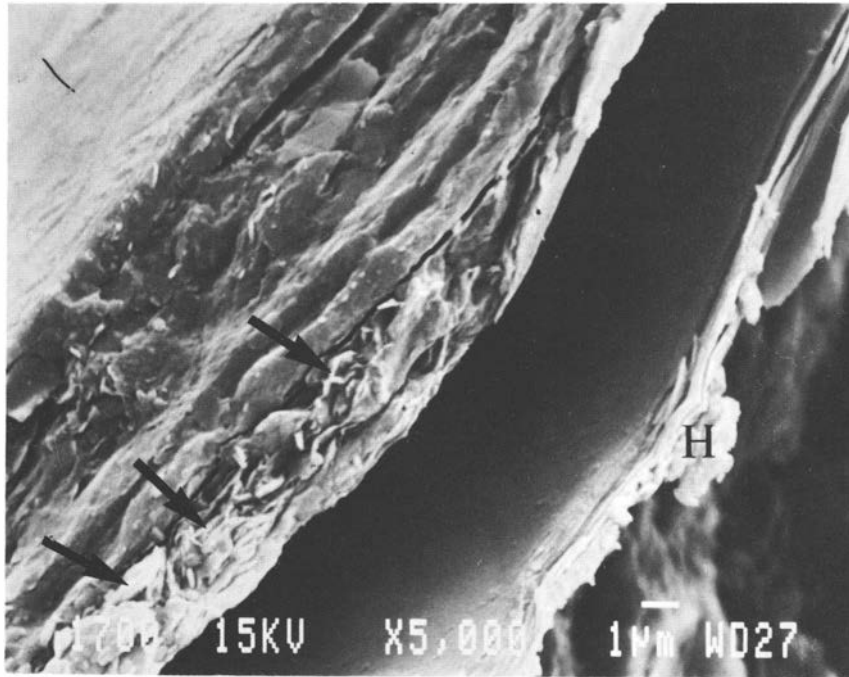


Fig. 3. A SEM micrograph showing a biotite grain partly replaced by clay mineral flakes (arrows) and hematite (H) in a shale sample from the distal-fan facies.

The positive correlation between MgO, FeO, and Al<sub>2</sub>O<sub>3</sub> in the RS and GS shales (Tables 3 and 4) indicates that Mg occurs mainly in the chlorite. The higher amounts of MgO in the GS shales than in the RS shales is related to the higher chlorite content in the former shales. The MgO and CaO contents are

highest in the ISS shales and the positive correlation between them (Table 5) suggests their presence mainly as carbonates. In the GS and RS shales CaO is positively correlated with Al<sub>2</sub>O<sub>3</sub> suggesting the occurrence of Ca mainly as plagioclase. The Na<sub>2</sub>O contents do not vary considerably between the shale

Table 2. Average chemical composition of the reddish alluvial-fan shales (RS; 16 samples), grey-green alluvial-fan shales (GS; 15 samples), and intertidal-subtidal shales (ISS; 21 samples).

		RS	GS	ISS
SiO <sub>2</sub>	(wt.%)	62.43±1.80	60.98±2.61	55.93±7.70
TiO <sub>2</sub>	(wt.%)	0.94±0.15	0.86±0.14	0.80±0.14
Al <sub>2</sub> O <sub>3</sub>	(wt.%)	16.70±0.93	17.25±1.27	15.37±2.72
Fe <sub>2</sub> O <sub>3</sub>	(wt.%)	4.49±1.24	2.53±0.67	2.13±1.12
FeO	(wt.%)	1.53±0.38	4.13±0.70	3.99±1.25
MgO	(wt.%)	1.42±0.53	2.11±0.60	2.57±1.48
CaO	(wt.%)	0.96±0.40	0.94±0.20	5.29±5.20
Na <sub>2</sub> O	(wt.%)	1.52±0.69	1.48±0.18	1.47±0.67
K <sub>2</sub> O	(wt.%)	3.36±0.78	3.77±0.39	3.15±0.88
Mn	(ppm)	350± 89	977±135	861± 358
Zn	(ppm)	59± 18	58± 25	67± 29
Ni	(ppm)	38± 11	32± 6	44± 17
Pb	(ppm)	29± 10	28± 16	32± 14
Cr	(ppm)	75±25	61±32	69±36
Sr	(ppm)	174± 70	189± 62	322±151
Ba	(ppm)	329±120	345±112	459±110

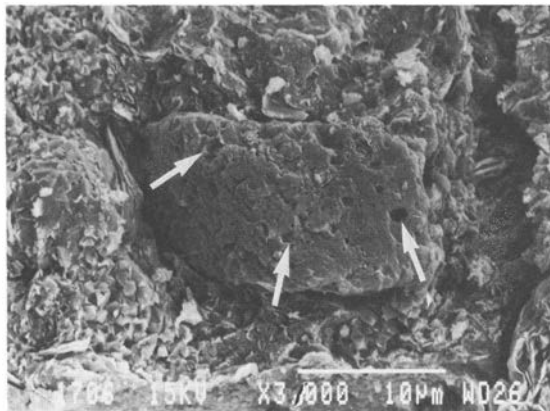


Fig. 4. A SEM micrograph showing a partly dissolved calcite intraclast (arrows) in a shale sample from the intertidal-subtidal facies.

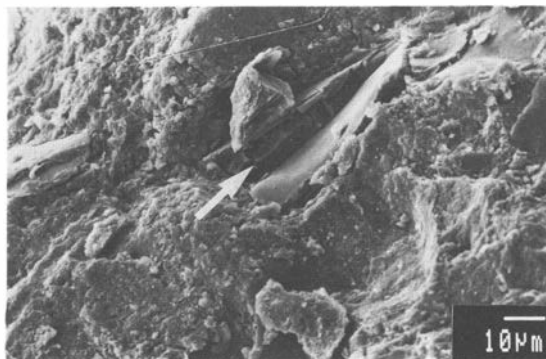


Fig. 6. A SEM micrograph showing that authigenic quartz has filled a micropore in a shale sample from the distal-fan facies.

groups due to the small variations in the plagioclase contents.

Chemical differences between the three shale groups are revealed from the trace element distribution too (Tables 3–5). Mn content is lower in the RS than in the GS and ISS shales (the latter two groups have similar Mn content). Mn substitutes for  $Fe^{2+}$  and Mg in chlorite and is thus more abundant in the GS than the RS shales. This is confirmed by the positive correlations between FeO, MgO, MnO and  $Al_2O_3$  (Tables 3 and 4). Table 5 reveals that Mn in the ISS shales is positively correlated with MgO and CaO indicating that Mn substitutes for Ca and Mg in the carbonates.

The Zn and Ni contents in the GS and RS shales are somewhat lower than in the ISS shales and are positively correlated with FeO,  $Fe_2O_3$ ,  $Al_2O_3$  and/or MgO (Tables 3–5) suggest that they occur in chlorite, illitic clay minerals and pyrite. The Pb content does not vary between the three shale groups and has a positive correlation with MgO and/or FeO in the GS and ISS shales suggesting that it occurs in chlorite and pyrite. In the RS shales, Pb is positively correlated with  $Fe_2O_3$  indicating its occurrence as hematite. The Cr content which differs slightly between the shale groups is positively correlated with  $Fe_2O_3$ ,  $Al_2O_3$  and  $K_2O$  (Tables 3 and 5) indicating its occurrence in illitic clay minerals and mica.

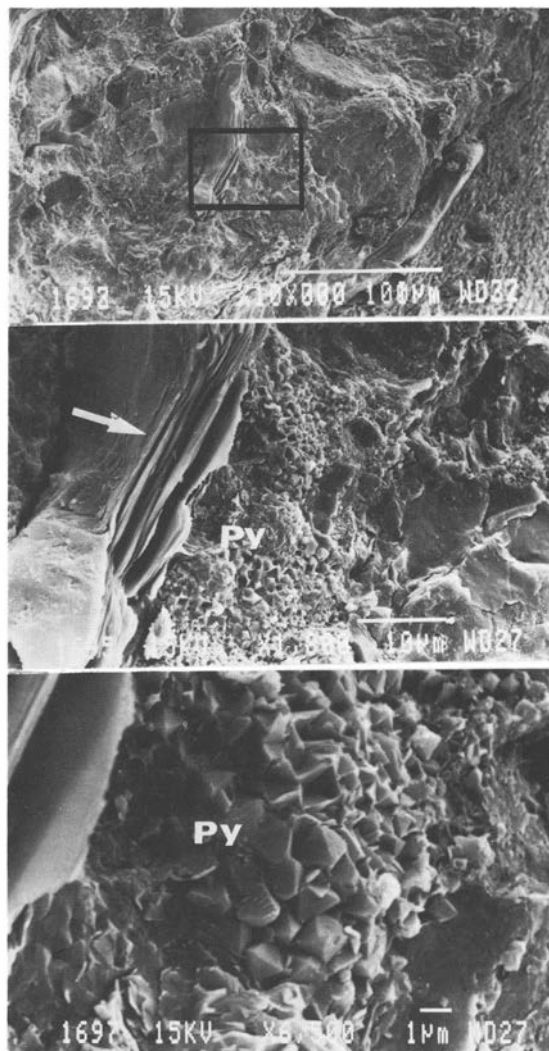


Fig. 5. (A) A SEM micrograph showing the occurrence of a biotite flake in a silty shale sample from the intertidal-subtidal facies. (B) A higher magnification of the area delineated in Fig. 5A showing the presence of authigenic pyrite (Py) close to the biotite flake (arrow). (C) The texture of pyrite (Py) in Fig. 5B shown at higher magnification. Notice the octahedral shape of the pyrite crystals.

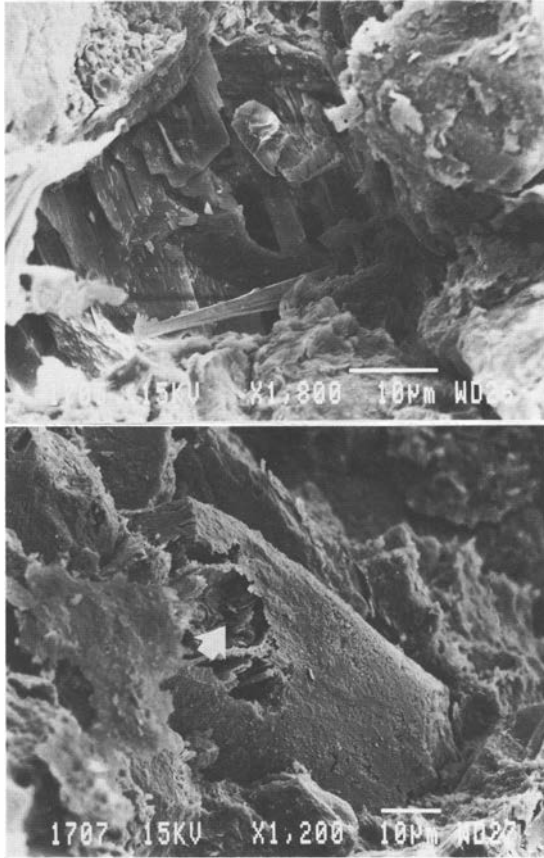


Fig. 7. SEM micrographs showing (A) partially dissolved feldspar and (B) partially dissolved and kaolinitized feldspar (arrow).

The Sr and Ba contents in the GS and RS shales are positively correlated with  $K_2O$  and  $Na_2O$  indicating their occurrence in feldspars. The average Sr and Ba contents are higher in the ISS shales than in the other two groups and are positively correlated with CaO and MgO indicating they reside in the carbonates too.

Some geochemical parameters of the Visingsö Group shales were compared with those of Archean to Phanerozoic shales studied by Schwab (1978). The Visingsö shales display a scatter when the  $SiO_2/Al_2O_3$  ratio vs  $Na_2O/K_2O$  ratio is plotted but mainly occur below the ranges for the Early to Late Proterozoic (Fig. 8). The Visingsö shales are depleted in  $SiO_2$  and  $Na_2O$  but have similar contents of  $FeO+Fe_2O_3+MgO+CaO+Na_2O$  compared to the Archean to Phanerozoic shales (Fig. 9). Depletion in  $SiO_2$  is apparently related to the finer grain size (more clay minerals) and lower amounts of quartz in the Visingsö samples compared to the sedimentary rocks of Schwab (1978).

#### Discussion and conclusions

The results presented in this study show that mineralogical and/or chemical differences between shales in a single sedimentary sequence might be controlled by depositional environment and/or diagenetic modifications. The colour of the shales is controlled by the redox potential of the pore solutions and is important during very shallow burial diagenesis. Under oxidising conditions, reddish colour forms due to stabilization of Fe-oxides/hydroxides

Table 3. Correlation matrix of chemical parameters of the reddish alluvial-fan shales.

	1	2	3	4	5	6	7	8	9	10	11	12	13	14	15	16
(1) $SiO_2$	1.00															
(2) $TiO_2$	-0.52	1.00														
(3) $Al_2O_3$	-0.55	0.56	1.00													
(4) $Fe_2O_3$	-0.68	0.58	0.51	1.00												
(5) FeO	-0.50	-	0.52	-0.58	1.00											
(6) MgO	-0.51	-	0.51	-0.56	0.59	1.00										
(7) CaO	-0.56	-	-	-	-	-	1.00									
(8) $Na_2O$	-	-	0.53	-	-	-	0.53	1.00								
(9) $K_2O$	-	0.55	0.61	0.52	-0.69	-0.75	-	-	1.00							
(10) Mn	-	-	-	-	0.54	0.50	-	-	-	1.00						
(11) Zn	-	-	-	-	-	0.54	0.50	-	-	-	1.00					
(12) Ni	-	-	-	-	-	0.50	-	-	-	-	-	1.00				
(13) Pb	-	-	0.53	0.58	-	-	-	-	0.56	-	-	0.76	1.00			
(14) Cr	-	-	0.53	0.54	-	-	-	-	-	-	0.52	-	-	1.00		
(15) Sr	-	-	0.54	-	0.50	-0.51	0.51	-	0.68	-	-	-	-	-	1.00	
(16) Ba	-	-	0.51	-	-	-	0.54	0.56	0.52	-	-	-	-	-	-	1.00

- means  $<0.50$  and  $<-0.50$

Table 4. Correlation matrix of chemical parameters in the grey-green alluvial-fan shales.

	1	2	3	4	5	6	7	8	9	10	11	12	13	14	15	16
(1) SiO <sub>2</sub>	1.00															
(2) TiO <sub>2</sub>	-0.61	1.00														
(3) Al <sub>2</sub> O <sub>3</sub>	-0.86	0.53	1.00													
(4) Fe <sub>2</sub> O <sub>3</sub>	-0.52	0.56	0.51	1.00												
(5) FeO	-0.68	-	0.50	-0.71	1.00											
(6) MgO	-0.63	-0.52	0.52	-0.65	0.85	1.00										
(7) CaO	-0.59	-	-	-0.53	0.51	-	1.00									
(8) Na <sub>2</sub> O	-	-	0.56	-	-	-	0.51	1.00								
(9) K <sub>2</sub> O	-0.53	0.54	0.59	0.70	-0.76	-0.70	-	-	1.00							
(10) Mn	-	-	0.53	-	0.50	0.53	-	-0.50	-	1.00						
(11) Zn	-	-	0.60	0.58	0.52	0.55	-	-	-	-	1.00					
(12) Ni	-	-	-	-	0.53	0.50	-	-	-	-	-	1.00				
(13) Pb	-	-	-	-0.51	0.55	0.54	-	-	-	-	-	0.54	1.00			
(14) Cr	-	-	-	0.54	-	-	-	0.66	-	-	-	-	-	1.00		
(15) Sr	-0.54	-	-	-	-	-	-	0.64	-	-	-	-	-	-	1.00	
(16) Ba	-0.52	-	-	-	-	-	0.52	0.53	-	-	-	-	0.60	0.51	-	1.00

- means <0.50 and <-0.50

mainly as fine pigment. These pigment can be of detrital or diagenetic origins. Conversely, grey-green and black colours in shale form under reducing conditions (cf. Thompson 1970; Van Houten 1972; Morad 1983). Reducing conditions enhance the dissolution of Fe-oxides and precipitation of dissolved Fe<sup>2+</sup> as pyrite, chlorite or carbonate (Berner 1981).

Formation of pyrite and carbonates as well as relatively abundant chlorite in shales of the upper unit reflect the influence of sediment diagenesis under marine environment (intertidal-subtidal). These minerals exerted a major influence in the dis-

tribution of elements in the shales. Mn, Mg, Sr, and Ba were incorporated in the carbonate whereas Fe was incorporated in the pyrite too. In the alluvial-fan shales, these elements occur mainly in the silicates.

As shown by figures 8 and 9 secular changes in composition of the Earth's upper crust cannot solely explain the variations in chemical composition of the Visingsö shales or the clastic sedimentary rocks presented by Schwab (1978). Instead, we believe that chemical compositions of clastic rocks are strongly controlled by grain size, depositional environment and diagenetic evolution path. For exam-

Table 5. Correlation matrix of chemical parameters in the intertidal-subtidal shales.

	1	2	3	4	5	6	7	8	9	10	11	12	13	14	15	16
(1) SiO <sub>2</sub>	1.00															
(2) TiO <sub>2</sub>	-	1.00														
(3) Al <sub>2</sub> O <sub>3</sub>	-	0.52	1.00													
(4) Fe <sub>2</sub> O <sub>3</sub>	-	-	-	1.00												
(5) FeO	-	-	-	-0.53	1.00											
(6) MgO	-0.76	-	-0.56	-	-	1.00										
(7) CaO	-0.78	-0.51	-0.56	-	-	0.50	1.00									
(8) Na <sub>2</sub> O	-	-	0.64	-	-	-	-0.50	1.00								
(9) K <sub>2</sub> O	-	-	0.62	-	-	-0.51	-	-	1.00							
(10) Mn	-	-	-	-	-	-	0.70	-	-	1.00						
(11) Zn	-	-	-	-	0.53	-	-	-	-	0.50	1.00					
(12) Ni	-	-	-	-	0.56	-	-	-	-	-	-	1.00				
(13) Pb	-	-	-	-	0.52	-	-	-	-	0.55	0.80	-	1.00			
(14) Cr	-	-	0.53	0.51	-	-	-	-	0.56	-	-	-	-	1.00		
(15) Sr	-0.79	-	-	-	-	0.51	0.93	-	-	0.68	-	-	-	-	1.00	
(16) Ba	-0.73	-	-	-	-	0.50	0.77	-	-	0.60	-	-	-	-	0.92	1.00

- means <0.50 and <-0.50

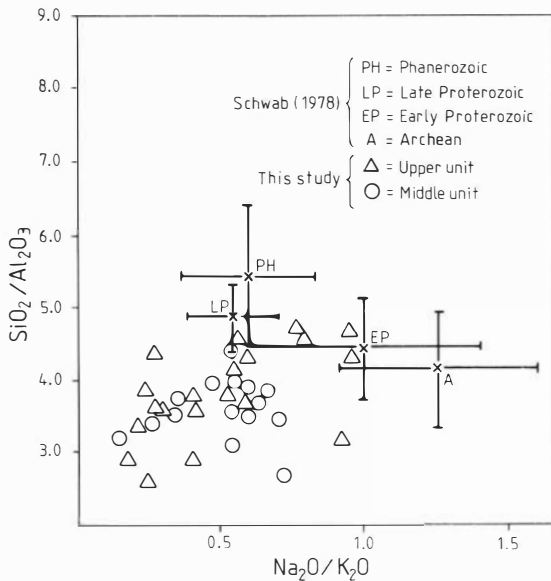


Fig. 8. A plot of the shale samples studied on a  $\text{SiO}_2/\text{Al}_2\text{O}_3$  ratio vs  $\text{Na}_2\text{O}/\text{K}_2\text{O}$  ratio diagram in order to compare their compositions with those of Archean to Phanerozoic sedimentary rocks (Schwab 1978).

ple, enrichment of shales in Na relative to K or Ca might be due to albitization of detrital potassium feldspar and plagioclase, respectively. Albitization of K-feldspar is common in the alluvial sandstones of the Visingsö Group (Morad 1986) but has not been detected in the shales. This might explain the lower  $\text{Na}_2\text{O}/\text{K}_2\text{O}$  ratio in the Visingsö shales (fig. 8) compared to the sedimentary rocks of Schwab (1978).

**Acknowledgements.** — A major part of the chemical analyses used in this study were made in the 1940's by the late Brita Collini. — We are grateful to Anne Marie Karlson for having performed many of the analyses. Christina Wernström kindly drafted the figures. The SEM work was conducted at the Agricultural University of Norway. The constructive review of the paper by the journal's referees Sven Snäll, Ulf Sturesson and Claes Ålinder is gratefully acknowledged. We thank Göran Granath for valuable comments. The Swedish Natural Science Research Council (NFR) funded the research.

## REFERENCES

- Blatt, H., Middleton, G. & Murray, R., 1980: *Origin of sedimentary rocks*. New Jersey, Prentice-Hall, 782 pp.  
 Caroll, D., 1958: Role of clay minerals in the transportation of iron. *Geochimica et Cosmochimica Acta* 14: 1–27.

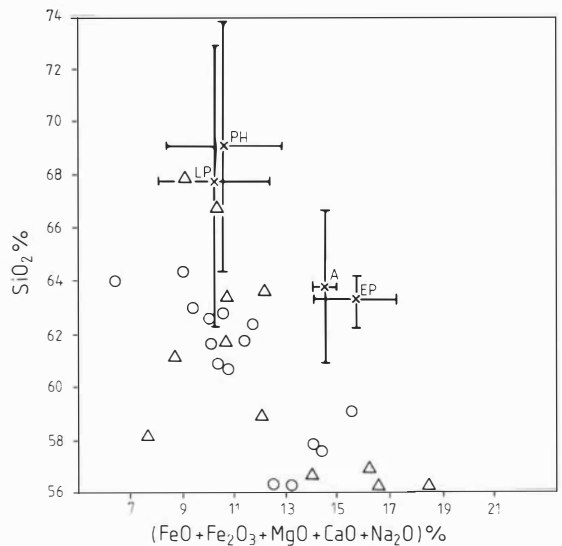


Fig. 9. The relationship between percentage of  $\text{SiO}_2$  and total percentage of  $\text{FeO}+\text{Fe}_2\text{O}_3+\text{MgO}+\text{CaO}+\text{Na}_2\text{O}$  in the Visingsö shales compared to the ranges found in Archean to Phanerozoic rocks (Schwab 1978). Symbols as in Fig. 8.

- Collini, B., 1951: Visingsöformationen, In P. Geijer, B. Collini, H. Munthe & R. Sandgren: *Beskrivning till Kartbladet Gränna. Sveriges Geologiska Undersökning Aa 193: 27–37*.  
 Hosterman, J.W. & Loferski, P.J., 1978: Preliminary report on the clay mineralogy of the Upper Devonian Shales in the northern and middle Appalachian basin. *United States Geological Survey, Open-File Report 78–1084*, 19 pp.  
 Kolthoff, I.M. & Sandell, E.B., 1959: *Textbook of Quantitative Inorganic Analysis*. New York, MacMillan, 759 pp.  
 Morad, S., 1983: Diagenesis and geochemistry of the Visingsö Group (Upper Proterozoic), southern Sweden: A clue to the origin of color differentiation. *Journal of Sedimentary Petrology* 53: 51–65.  
 Morad, S., 1986: Albitization of K-feldspar grains in Proterozoic arkoses and greywackes from southern Sweden. *Neues Jahrbuch für Mineralogie, Monatshefte* 1986: 145–156.  
 Morad, S. & AlDahan, A.A., 1986: Alteration of Fe-Ti oxides in sedimentary rocks. *Bulletin of the Geological Society of America* 83: 2761–2772.  
 Schwab, F.L., 1978: Secular trends in composition of sedimentary rock assemblages — Archean through Phanerozoic time. *Geology* 6: 532–536.  
 Thompson, A.M., 1970: Geochemistry of color genesis in red-bed sequence, Juniata and Bald Eagle Formation, Pennsylvania. *Journal of Sedimentary Petrology* 40: 599–615.  
 Van Houten, F.B., 1972: Iron and clay in tropical savannah alluvium, A contribution to the original of red beds. *Bulletin of the Geological Society of America* 97: 567–578.